Scientific Research Publishing

Materials Sciences and Applications, 2022, 13, 491-505
https://www.scirp.org/journal/msa
ISSN Online: 2153-1188
ISSN Print: 2153-117X

Electrical Properties of Compositional Al_2O_3 Supplemented HfO_2 Thin Films by Atomic Layer Deposition

Yuxi Wang[1,2,3], Yong Zhang[1,2,3], Tingqu Wu[4], Weizheng Fang[4], Xufeng Kou[1], Tao Wu[1], Jangyong Kim[1,4*]

[1]School of Information Science and Technology, ShanghaiTech University, Shanghai, China
[2]Shanghai Institute of Microsystem and Information Technology, Chinese Academy of Sciences, Shanghai, China
[3]University of the Chinese Academy of Sciences, Beijing, China
[4]ShanghaiTech Quantum Device Laboratory, ShanghaiTech University, Shanghai, China
Email: *jangyongkim@shanghaitech.edu.cn

How to cite this paper: Wang, Y.X., Zhang, Y., Wu, T.Q., Fang, W.Z., Kou, X.F., Wu, T. and Kim, J.Y. (2022) Electrical Properties of Compositional Al_2O_3 Supplemented HfO_2 Thin Films by Atomic Layer Deposition. *Materials Sciences and Applications*, **13**, 491-505.
https://doi.org/10.4236/msa.2022.139030

Received: March 12, 2022
Accepted: September 16, 2022
Published: September 19, 2022

Copyright © 2022 by author(s) and Scientific Research Publishing Inc.
This work is licensed under the Creative Commons Attribution International License (CC BY 4.0).
http://creativecommons.org/licenses/by/4.0/

Open Access

Abstract

With advanced research for dielectrics including capacitors in DRAMs, decoupling filters in microcircuits and insulating gates in transistors, a lot of demand for the new challenging of high-*k* materials in semiconductor industries has been emerged. This study explores and addresses the experimental approach for composite materials with one of the major concerns of high capacitance, and low leakage, as well as ease of integration technology. The characteristics of Al_2O_3 supported HfO_2 (AHO) thin films for a series of different Hf ratios with Al_2O_3 dielectrics by atomic layer deposition demonstrated as a candidate material. A composite AHO films with the homogeneous compositions of Al and Hf atoms into the Al-Hf-O mixed oxide system could stabilize the polycrystalline structure with increasing of dielectric constant (*k*) and decreasing of leakage current density, as well as a higher breakdown voltage than HfO_2 film on its own. 70 nm thick AHO thin films with different composition of Al and Hf contents were prepared by atomic layer deposition technique on titanium nitride (TiN) and silicon dioxide (SiO_2) coated Si substrates. Photolithography and metal lift-off technique were used for the device fabrication of the metal-insulator-metal (MIM) capacitor structures. AHO films on $TiN/SiO_2/Si$ were measured by semiconductor analyzer and source/measure system with probe station in the voltage range from −5 to 5 V with a frequency range from 10 kHz to 1 MHz were used to conduct capacitance-voltage (C-V) measurements with low/medium frequency range and current-voltage (I-V) measurements. It was found that $Au/AHO/TiN/SiO_2/Si$ MIM capacitors demonstrate a capacitance density of 1.5 - 4.5 fF/μm^2 at 10 kHz, a

loss tangent of 0.02 - 0.04 at 10 kHz, dielectric constant of 11.7 - 35.5 depending on the composition and a low leakage current of 1.7×10^{-9} A/cm^2 at 0.5 MV/cm at room temperature. The acquired experimental results could show the possibility of compositional alloy thin films that could potentially replace or open new market for high-*k* challenges in semiconductor technology.

Keywords

High-*k* Dielectrics, Hafnium Oxide, Aluminium Oxide, Composites, Thin Film Capacitors, Atomic Layer Deposition, Microfabrication

1. Introduction

With the continuous improvement of integrated circuit (IC) design, the research of high-*k* (high dielectric constant) materials has received considerable attention [1]. For microelectronics industry, it is necessary to have high performance and low cost devices, so the number of devices on single chip is very important. At the same time, the size of devices is required to be smaller [2] and the miniaturization of complementary metal-oxide-semiconductor (CMOS) field-effect transistors has inspired a major push to study alternative gate oxide materials with higher dielectric constants and replace silicon dioxide (SiO_2) [3] [4] [5]. Due to the existence of quantum tunneling effect, when the photolithography linewidth is less than 0.1 μm, the gate oxide layer thickness gradually approaches the atomic spacing, resulting in unacceptable leakage current and thermal loss [6]. Therefore, high-*k* materials are introduced to replace the traditional gate dielectric SiO_2. It is ensure that the gate dielectric layer has enough physical thickness while maintaining and increasing the gate capacitance, to solve the leakage current caused by direct tunneling.

Binary metal-oxide dielectrics with high dielectric constant have recently been gaining exponential interest, performing a leading role in the replacement of gate dielectrics for CMOS devices. Hafnium oxide (HfO_2) is technologically important material due to its high dielectric constant ($k = 20$ - 25), high bulk modulus, great thermal stability, high melting point, low crystallization temperature, high chemical stability on the surface of Si, and moderate band gap (5.5 - 6.0 eV). The trade-off, however, is its fundamental problems that is particularly related with the poor thermal stability, undesirable crystallinity, poor interface with Si, high interface state density, high leakage current, and high oxygen diffusion through the HfO_2 that need to be resolved for CMOS application [7] [8] [9]. On the other hand, aluminium oxide (Al_2O_3) has a good insulate properties, relatively large bandgap (E_g~8.8 eV), band alignment likeness to SiO_2, attractive thermal stability, excellent chemical stability, high mechanical strength, high electric field strength, reduction of oxygen transport, high-temperature resistivity, and high conduction band offset to semiconductor substrates, but it has strug-

gled with relatively low dielectric constant (k~9) [10] [11] [12] [13] [14].

Recently, several research groups have studied the substitution of aluminum into binary high-k materials to decrease leakage current levels and improve the thermal stability. The naturally combined Al_2O_3 and HfO_2 in the form of alloy and/or layered structures have been investigated as alternative high-k materials and its possibly achievable lower leakage current and large bandgap characteristics depending on the mixture ratio [15]-[21]. However, Al inclusion in $HfAl_xO_y$ has also been reported in the fixed or narrow range of concentrations indicating relatively complicated crystalline structures and causing a poor electrical property with low k value. Laminated structure of HfO_2-Al_2O_3 has also been reported for different research, all of them were showing excellent leakage characteristics and good device reliability [12] [13] [14]. Following the demand of dielectric layers, thermal stability, structural and electrical properties of the modulated HfO_2/Al_2O_3 films fabricated with various deposition technique have previously investigated by many other groups. However, it has been reported in the fixed or narrow range of compositions, the complicated crystalline structures, the poor descriptions for experimental process and the relatively low electrical property with unclear composition. It seems to be valuable to study the composite of Al-Hf-O system to improve the electrical properties of high-k dielectric materials, which is one of the promising strategy in further miniaturization of microelectronic components.

In this report, we taking aim at the growth of Al_2O_3 supplemented HfO_2 (AHO) thin films with a different aluminum and hafnium compositional range on Si substrates by atomic layer deposition (ALD) technique and the experimental investigation of compositional effect on their structural and electrical properties of thin film capacitors. The measurement of capacitance as function of DC voltage at low/medium frequency range and leakage current as function of electric field amplitude is carried out. The investigation of structure and surface morphology with different Al and Hf concentration is also performed to support the optimum electrical properties of composite films and the improvements of performance for the next generation of metal-insulator-metal (MIM) capacitors.

2. Materials and Devices Fabrication

The deposition of AHO thin films were grown on 500 μm thick silicone single crystal substrates with ALD system (*PICOSUN^{TM} R-200 Advanced*). Before AHO film deposition, 500 nm thick SiO_2 was deposited directly on Si substrates by Plasma Enhanced Chemical Vapor Deposition (PECVD) after removing of native oxide on the Si sur-face using dilute hydrofluoric acid (HF) containing Buffered Oxide Etch (BOE) solution for 2 minutes. For bottom electrode, titanium nitride (TiN) with the thickness of 50 nm was deposited at 400˚C by Plasma-Enhanced ALD (PEALD) on SiO_2 (500 nm)/Si substrates, using $TiCl_4$ as Ti precursor and NH_3 as N plasma gas. The plasma power and NH_3 gas flow rate

were 2500 W and 150 sccm, respectively. Subsequently these substrates were kept in the ALD chamber without vacuum break for immediate next deposition step.

AHO thin films were grown at 370˚C with a background pressure of 200 mTorr by thermal ALD process on TiN(50 nm)/SiO_2(500 nm)/Si substrates using trimethyl aluminium (TMA) as Al precursor, tetrakis dimethyl amino hafnium (TDMAHf) as Hf precursor, and water vapor (H_2O) as O_2 precursor. Four AHO composite film samples were prepared using alternating TMA-H_2O (Al_2O_3) and TDMAHf-H_2O (HfO_2) reaction cycles for the control of different composition, where all deposition started with Al_2O_3 to improve the interface quality [22]. The control of composition was carried out by pulsing one Al_2O_3 sub cycle every one, two, three, or four HfO_2 sub cycles. The total number of super cycles was varied in the range from 110 to 300 and adjusted by calculated growth rate of individual Al_2O_3 and HfO_2 depositions to keep a similar thickness level. Detailed information about deposition conditions are summarized in **Table 1**.

The thickness of as grown films were determined by surface profilometer (*Bruker DektakXT*) with the growth rates of 0.12 - 0.14 nm/cycle. Scanning Electron Microscopy (SEM) with cross sectional samples were used to double check the thickness of all layers which has no significant variations of deposition rates. Optimum growth recipes for AHO composite films by ALD deposition was based on the individual Al_2O_3 and HfO_2 growth conditions, which are summarized in **Table 2**.

Photolithography and metal lift-off technique were employed for the fabrication of a complete electrode patterns directly on AHO films to define MIM capacitors. AHO film samples were cleaned using acetone within an ultrasonic vibrator for 5 minutes, then rinsed in isopropanol (IPA) and de-ionized (DI)

Table 1. ALD deposition conditions of AHO films.

Sample	Composition (At %)		Sub cycles		Super cycles	Growth Rate (nm/cycle)
	Al	Hf	Al_2O_3	HfO_2		
AHO[1/1]	63	37	1	1	300	0.12
AHO[1/2]	43	57	1	2	200	0.14
AHO[1/3]	33	67	1	3	140	0.13
AHO[1/4]	21	79	1	4	110	0.13

Table 2. ALD deposition conditions of Al_2O_3 and HfO_2 films respectively.

Sample	Temperature (˚C)	Carrier Gas (sccm)			Pulse (s)			Purge (s)		
		TMA	TDMAHf	H_2O	TMA	TDMAHf	H_2O	TMA	TDMAHf	H_2O
Al_2O_3	370	150	-	200	0.1	-	0.1	4.0	-	6.0
HfO_2	370	-	100	150	-	1.6	0.1	-	5.0	1.0

water, and finally dried with nitrogen to remove atmospheric dust and contamination. Cleaned sample should be prebaked at 110˚C for 2 minutes for drying of water vapor. Optionally the sample was placed in an HMDS (Hexamethyldisilazane) environment for 2 minutes to make good adhesion between film and photoresist layer. Photoresist (*Clariant AZ5214E*) with a thickness of ~1.4 μm was spin-coated on the top surface of AHO/TiN/SiO_2/Si samples with the speed of 4000 rpm for 30 s and then baked on a hot plate at 95˚C for 1 minute to act as a photosensitive polymer and pattern exposure. Maskless Aligner (*Heidelberg Instruments MLA150*) system was used for UV lithography with a dose of 170 mJ/cm^2 and a wavelength of 405 nm. After exposure, the pattern was developed at room temperature for 50 s in a solution composed of developer (*Microposit 351*) and DI water with the ratio of 1:5. The sample was rinsed with DI water for 30 s to stop the development and clean the sample surface followed by N_2 blowing for sample dry. Ion Beam Etching (IBE) was used for the opening of bottom electrode with a 2 μm thick photoresist mask before lithography process. The etching rate of AHO film was approximately 30 nm/min.

The metal deposition was performed by electron-beam evaporation (*Explorer Coating System*, *Denton Vacuum*) under high vacuum conditions of 2×10^{-7} Torr. The electrodes consisted of a thin layer of Ti (10 nm) acting as an adhesive layer between thin film and top electrodes covered by a thicker layer of Au (130 nm) that has its high conductivity and oxidation resistance. In the lift-off process, the sample was put in an ultrasonic acetone bath for about 10 minutes, thereafter rinsed in isopropanol for about 3 minutes and DI water, and finally dried with nitrogen to remove the resist and unwanted metal. The diameters of top electrodes were in the range of 100 - 500 μm in any individual device. The pattern for electrical characterization consists of an array of circular electrodes for MIM capacitor structures is shown schematically in Figure 1.

3. Measurements

AHO thin film with different composition was measured by Energy-Dispersive X-ray Spectrometer (EDX) to confirm elemental distribution (atom %) of Al, Hf and O, on multi-mode Scanning Electron Microscopy (SEM, *Carl Zeiss Gemini 300*) with optional EDX detector (*RemCon32/RS232*). EDX spectra can classify

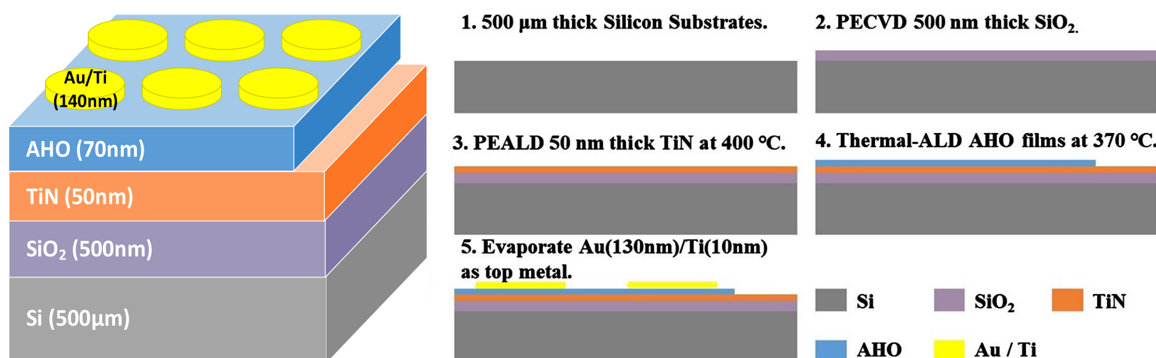

Figure 1. Schematic of sample structure and device fabrication process.

minerals based on the mineral stoichiometry and produce mineral map. Additional scan modes and image processing allowed flexible analysis and ability to target areas and phases of interest. Subsequently, the surface morphology of AHO thin film was examined by atomic force microscope (AFM) on Dimension Icon (*Bruker iCON*) operated in scanning non-contact mode. The physical thickness of each AHO thin film was measured with surface profilometer and was found to be approximately 70 nm. X-ray diffraction (XRD) measurement with θ-2θ scan was performed in the areas of AHO thin film to get the information about crystalline orientation of the material in the growth direction depending on the different sub cycles of HfO_2. Empyrean multi-purpose X-ray diffractometer (*Malvern Panalytical*) with the wavelength of the incident Cu-Kα radiation source, equal to λ = 1.54056 Å (40 kV, 30 mA). The θ-2θ scan was performed over of wide angular range from 20˚ to 80˚ with 0.04˚ steps and a 20 s counting time.

To qualify the dielectric properties in vertical capacitive MIM structure, the capacitance (C)-voltage (V) and current (I)-voltage (V) characteristics were measured by programmable Semiconductor Analyzer (*Keysight B1500A*) and by Precision Source/Measure system (*Keysight B2912A*), respectively. Measurements were done connecting the TiN plain bottom electrode as the ground and the Au top electrode as the biasing. Various DC bias voltages from −5 V to 5 V was applied to the vertical capacitive structure using the microprobe in the probe station (*FormFactor MPS150*) with the internal bias tees of Semiconductor analyzer. Measurements were carried out with a continuous voltage ramp and each different frequency (10 kHz, 50 kHz, 100 kHz, 500 kHz, and 1 MHz), where current was measured at the end of each voltage step. A single expression for the capacitance of infinite flat capacitors $C = \varepsilon_0\varepsilon_r(A/d)$, where the ε0 is the permittivity of vacuum ($\varepsilon_0 \sim 8.854 \times 10^{-12}$ F/m), A is the area of the capacitor, and d is the distance between the capacitor electrodes, was employed for the calculation of relative dielectric constant (ε_r). Real capacitance consists of the ideal capacitance component and the conductive component which can be expressed as a dielectric loss ($\tan\delta = G/\omega C$). Thus the dielectric loss has close relationship with leakage current in the capacitor structure and characterized by loss angles as well as by capacitance. Good dielectrics quoted as a figure of merit of capacitor since the loss angles are very small and nearly constant over a wide range of frequencies.

4. Results and Discussion

4.1. XRD Measurement

The XRD measurements with respect to the different composition of Hf element in the AHO film on TiN/Si substrates was performed to check growth quality. In Figure 2, preferentially (200)-oriented AHO films were obtained with very low intensity and small change of peak position as increase the number of unit cycles in a HfO_2 sub cycles from 1 to 4.

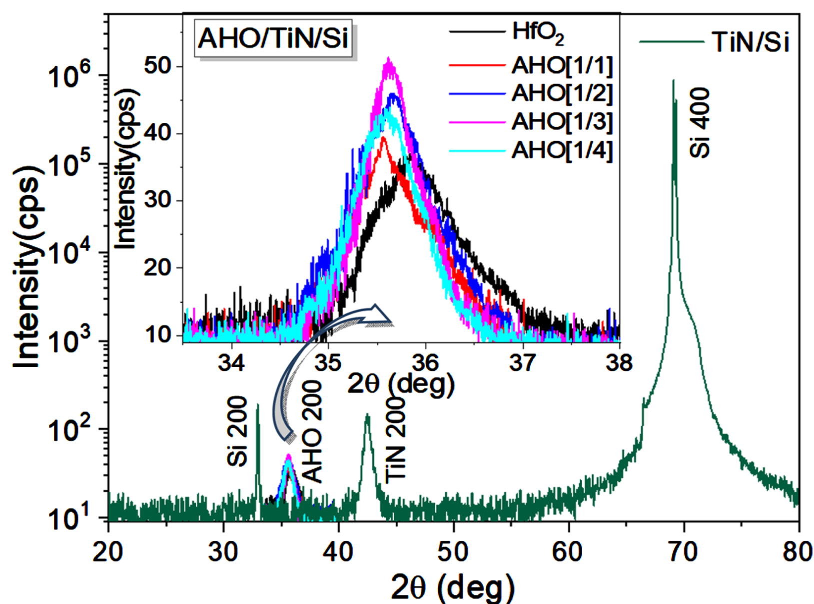

Figure 2. Broad range XRD θ-2θ patterns for AHO films on TiN/Si substrates (main figure) and the magnification of (200) peaks for AHO films on TiN/Si substrates compare with pure HfO_2 film (the inset).

A superimposed view of XRD patterns for AHO films in the inset of Figure 2 could be observed a shift of the peak position towards smaller 2θ values compare with binary HfO_2 film. This could be due to the interstitial addition of Al atoms with a smaller atomic radius to the Hf atoms with a larger atomic radius in the HfO_2 lattice which causes the lattice parameter of AHO films to increase in accordance with an increase in the volume of the unit cell [23]. However, the shifts observed between each peak still in the range of measurement error due to a calibration artefact. Therefore, 2θ scans with low intensity and diffused reflections could no show perfect crystallinity and complementary studies with reciprocal mapping would be needed for the proof of growth quality. As a supportive information, the AHO[1/3] film (67 At% of Hf concentration) with higher intensity might be considered for the best sample of dielectric properties in this report.

4.2. Surface Analysis

To view the material composition of the samples, EDX spectrometry was performed on the thin film samples for the elemental analysis. Figure 3 clearly shows a mapping of EDX signals for the atomic composition of thin films with different number of unit cycles in a HfO_2 sub cycles. As HfO_2 sub cycles increased from 1 to 4, elemental distribution (atom %) of Hf atoms shows from 37 to 79 as summarized in Table 1. In Figure 3, the Al and Hf signals are strong enough and clearly discernible, indicating that all the materials seem to be homogeneous and no impurities. It is understandable that the number of counts obtained during the EDX signals corresponds to the material composition used in the device fabrication.

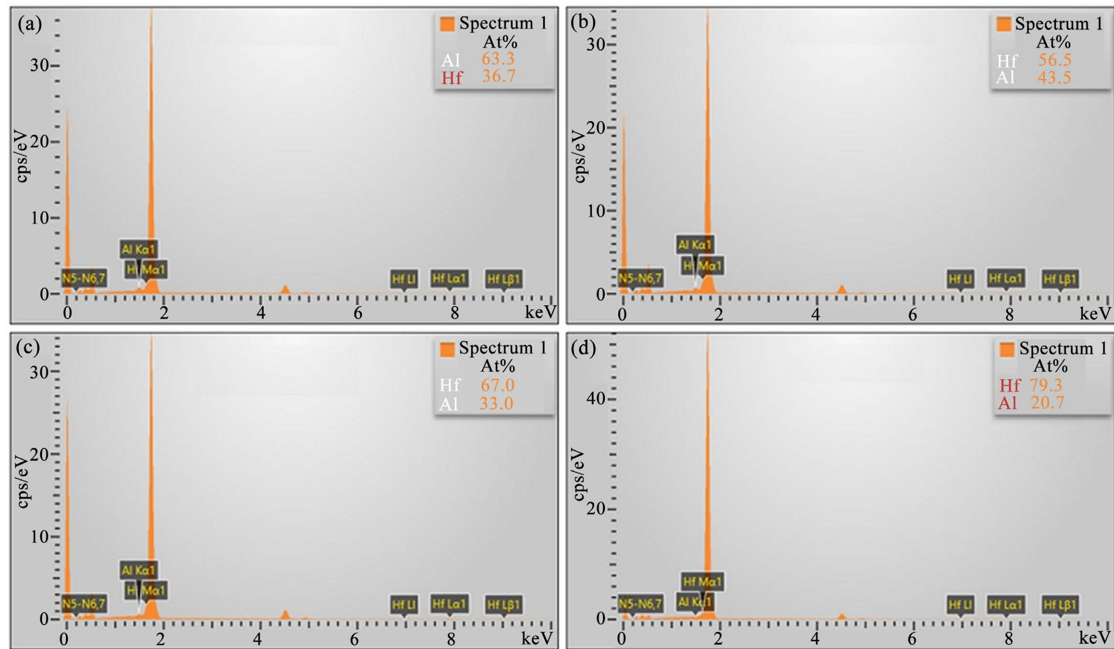

Figure 3. EDX spectrum of the fabricated AHO thin film samples for the analysis of the presence of Al and Hf composition in the samples. (a) AHO[1/1]; (b) AHO[1/2]; (c) AHO[1/3]; (d) AHO[1/4].

Figure 4 shows the AFM morphology investigation of as grown AHO films in comparison with the binary HfO_2 and Al_2O_3 films deposited on TiN/Si substrates. TiN films deposited on Si substrates shows microstructure with small particles growing and gathering in high temperature, which could induce the rougher surface as increase the crystallization. Therefore, all the films on TiN/Si substrates show little rougher RMS value from 1.68 to 7.40 nm compare with the similar group IV metal oxide films on various substrates with lower temperature [21] [24].

The root-mean-square (RMS), average roughness R_a and maximum roughness R_{max} calculated from topographic AFM image of as grown each films are summarized in **Table 3**. This appears considerably larger roughness with varying Hf concentration as increase of the number of unit cycles in a HfO_2 sub cycle. RMS and R_a is increased as the Hf concentration increased but R_{max} is suddenly down at AHO[1/3] sample (67 At% of Hf concentration) which could exercise a minor-reaching influence in the dielectric properties. The surface roughness and grain size of the dielectric layer may become another key feature influencing the efficiency of electrical properties in MIM capacitors. It is a common knowledge that dielectric constant continuously increases when grain size and surface roughness decreases up to a certain critical size and then decreases again below a critical grain size [25]. The critical grain size would vary with chemical composition of these dielectrics as well as with the route of synthesis of thin films and subsequent device fabrication. The experimental investigation of compositional effect on the dielectric properties of the AHO[1/3] sample with a 33/67 Al/Hf At% composition were more focused in electrical characterization.

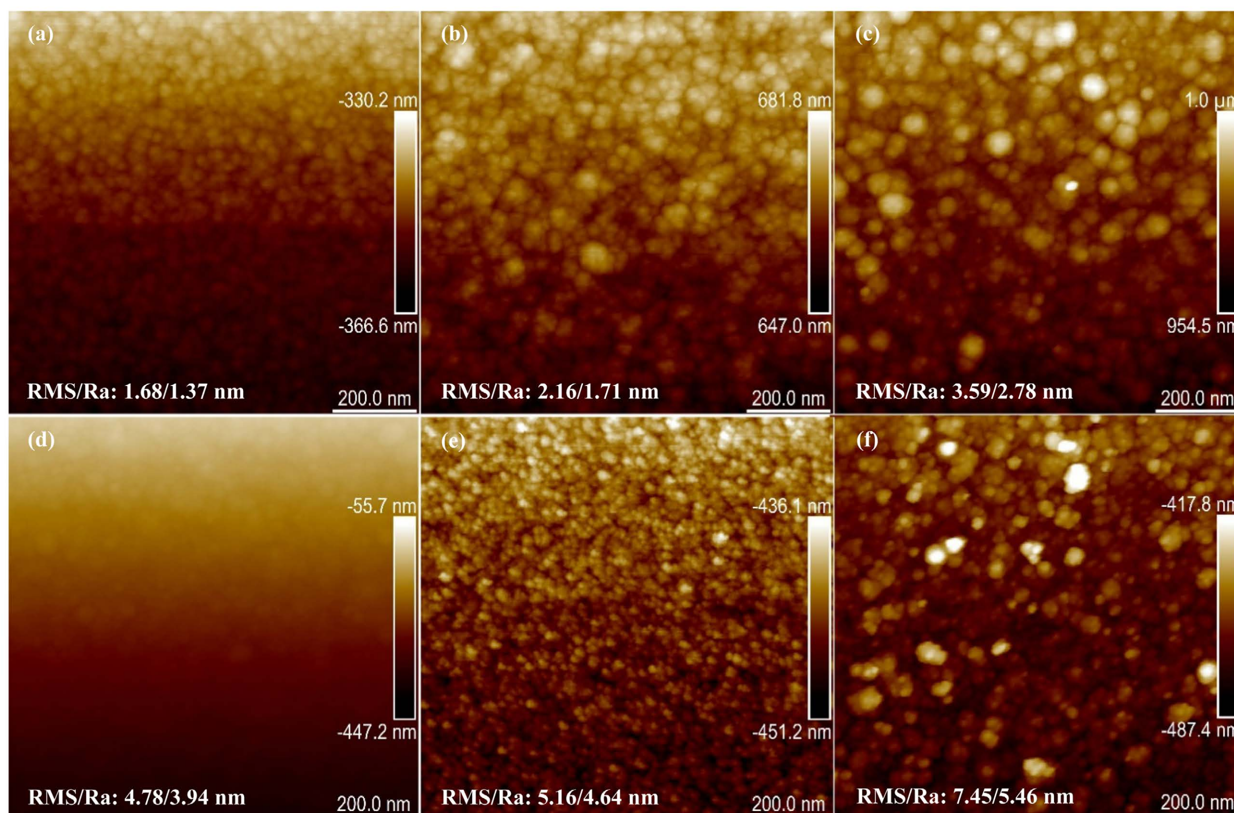

Figure 4. Topographic AFM image, 1 µm × 1 µm, with RMS roughness and average roughness of the films on TiN/Si deposited by ALD technique (a) Al_2O_3/TiN/Si; (b) AHO[1/1]/TiN/Si; (c) AHO[1/2]/TiN/Si; (d) AHO[1/3]/TiN/Si; (e) AHO[1/4]/TiN/Si; (f) HfO_2/TiN/Si.

Table 3. Summary of RMS, R_a and R_{max} calculated from AFM image.

Sample	RMS (nm)	R_a (nm)	R_{max} (nm)
Al_2O_3	1.68	1.37	11.3
AHO[1/1]	2.16	1.71	16.9
AHO[1/2]	3.59	2.78	32.9
AHO[1/3]	4.78	3.94	29.1
AHO[1/4]	5.61	4.64	33.7
HfO_2	7.45	5.46	58.3

4.3. Electrical Characterization

Capacitance vs. applied voltage (C-V) measurement was performed for Au/ AHO/TiN/SiO_2/Si MIM capacitors in the frequency range from 10 kHz to 1 MHz. A DC bias voltage is applied from −5 V to 5 V between the 200 µm cylinders shape Au electrode (top) and TiN flat electrodes (bottom). C-V single sweep was operated for each frequency point (10 kHz, 50 kHz, 100 kHz, 500 kHz, and 1 MHz). The capacitance densities and dielectric constant can be calculated from C-V measurements shown in **Figure 5** and plotted with varying Al

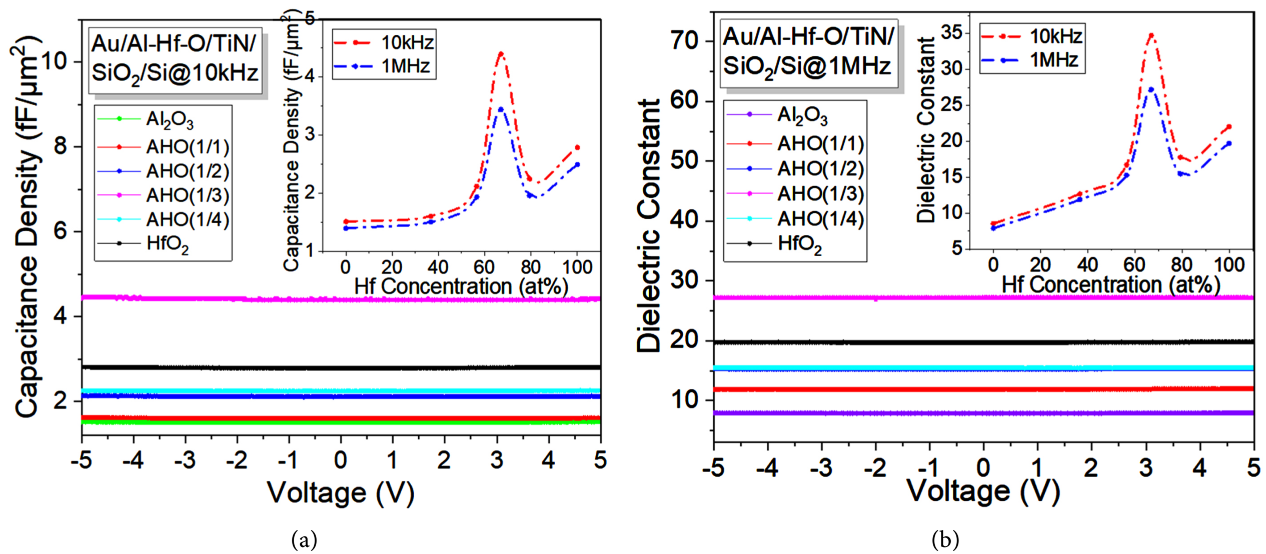

Figure 5. C-V characteristics of Al_2O_3 supplemented HfO_2 thin film as a function of the DC bias voltage for different frequencies: (a) Voltage dependence of capacitance density for AHO films with different Al and Hf compositions and capacitance density (inset) on the Hf concentration in AHO films at 10 kHz (red circles) and 1 MHz (blue circles); (b) Voltage dependence of dielectric constant for AHO films with different Al and Hf compositions and dielectric constant (inset) on the Hf concentration in AHO films at 10 kHz (red circles) and 1 MHz (blue circles).

and Hf composition of AHO films at certain frequency shown in **Figure 5** (inset). The stability of the capacitor is appeared to indicate the constant value of capacitance densities and dielectric constant at a fixed frequency in the continuously increasing DC voltage.

It is obtained that the capacitance density and relative dielectric constant for Al_2O_3 is around 1.2 - 1.5 fF/μm^2 and 7.9 - 8.5 at 10 kHz - 1 MHz respectively which is in very good agreement with our previous experiments. [26]. The pure HfO_2 film on $TiN/SiO_2/Si$ exhibits capacitance density and relative dielectric constant of 2.5 - 2.9 fF/μm^2 and 20 - 23 at 10 kHz - 1 MHz respectively that is close to theoretical value (1.55 fF/μm^2, 23.9 with cubic phase) found in literature [27]. In case of AHO films where the addition of Hf concentration has increased the dielectric constant as the number of unit cycles increasing in a HfO_2 sub cycle. A higher capacitance density and dielectric constant up to 4.5 fF/μm^2 and 35 at 10 kHz was observed in AHO film with a 33/67 Al/Hf At% composition when the applied electric field varied from −70 to 70 MV/m, which indicate excellent dielectric characteristics with regard to frequency. This result is at least half as much again as the value of HfO_2 film, which exhibits a strong directional anisotropy with high dielectric constant [28] [29]. It could be attributed to the preferred a-axis orientation and increased the molar volume in the composite films that was previously reported in the similar structure of Al_2O_3 added Ta_2O_5 films [30] [31].

Current vs. applied voltage (I-V) measurement was performed for Au/AHO/$TiN/SiO_2/Si$ MIM capacitors with a DC bias voltage from −5 V to 5 V. The current densities can be calculated from I-V measurements shown in **Figure 6** and plotted with varying Al and Hf composition of AHO films shown in

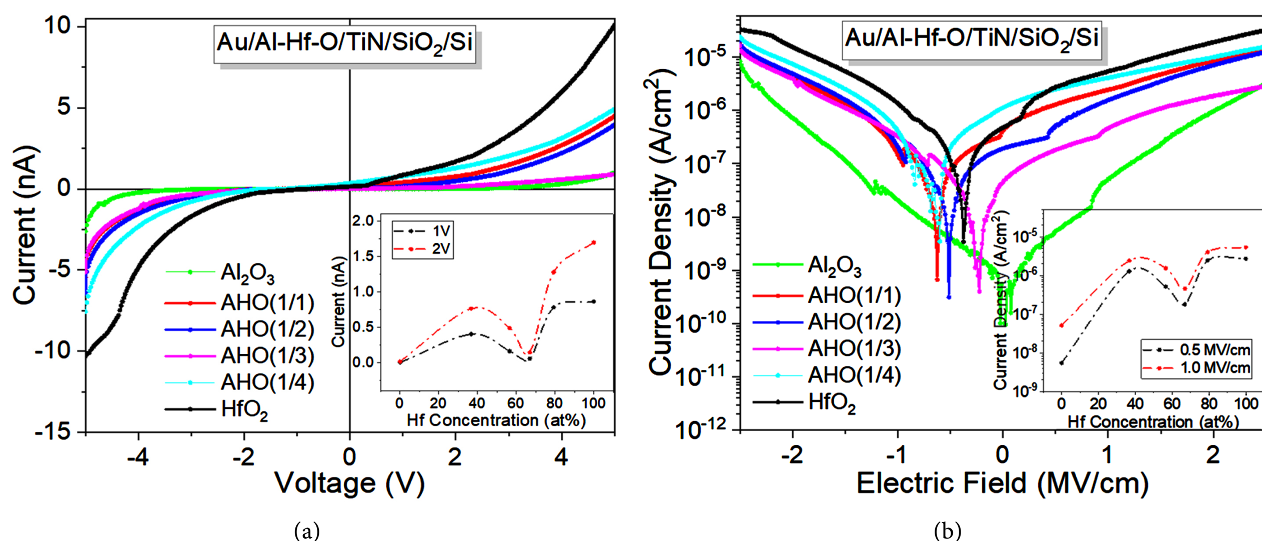

(a) (b)

Figure 6. I-V characteristics of Al_2O_3 supplemented HfO_2 thin film as a function of the DC bias voltage: (a) Voltage de-pendence of leakage current for AHO films with different Al and Hf compositions and leakage current (inset) on the Hf concentration in AHO films at 1 V (black circles) and 2 V (red circles); (b) Electric filed dependence of leakage current density for AHO films with different Al and Hf compositions and leakage current density (inset) on the Hf concentra-tion in AHO films at 0.5 MV/cm (black circles) and 1 MV/cm (red circles).

the inset of Figure 6. Since the conduction mechanism is based on the activation from electrons or holes with the thickness of 60 - 70 nm dielectrics in MIM structures, the quantum phenomenon has not been considered in this report.

It is noticed that forward leakage current causing bottom electrode injection becomes sharp increasing before 2 V because of different work function of the top and bottom electrode which were affected by the materials shown in Figure 6(a). On the other hand, reverse leakage current causing top electrode injection becomes smooth changing little over −2 V. This result demonstrates that the electron injection efficiency at the bottom interface larger than the one from the top electrode due to the work function of TiN (~4.3 eV) is smaller than that of Au (~5.3 eV) regardless of the type of current conduction. In Figure 6(b), the leakage current density of pure Al_2O_3 film on $TiN/SiO_2/Si$ is about 1.79×10^{-8} A/cm^2 at 1 MV/cm. In the composited film, leakage cur-rent increased up to 4.08×10^{-6} A/cm^2 at 1 MV/cm as increase of Hf concentration which is close to the leakage of pure HfO_2 film (~5.04×10^{-6} A/cm^2 at 1 MV/cm). However, lea-kage fairly decrease down to 4.61×10^{-7} A/cm^2 at 1 MV/cm with the Al/Hf composition of 33/67 At% in room temperature which indicates probably the best data as a composite dielectric layer compared with other laminated mate-rials. However, more complementary studies of electrical properties with the correlation of fundamental material compositions and structure properties in a real device behavior still in progress.

5. Conclusions

Al_2O_3 supplemented HfO_2 thin film MIM capacitors were fabricated by using ALD technique with precise control of material compositions onto TiN/SiO_2

deposited Si (100) single crystal substrates. Very weak (200) orientation of AHO films were observed by θ - 2θ scans of X-ray diffraction measurement. Material composition of the fabricated thin films clearly observed by EDX spectrometry with the elemental analysis of Al and Hf composition in the samples. Surface morphology studies for the AHO films deposited on TiN-coated Si substrates were performed by AFM measurements to understand the relationship between dielectric properties and thin film surface roughness, which can be caused by the bottom electrode surface roughness. Dielectric properties of AHO films on TiN/SiO_2/Si were carried out using semiconductor analyzer with probe station for a DC voltage sweep from −5 V to 5 V and fixed frequency points from 10 kHz to 1 MHz. Leakage current characteristics of MIM capacitors have been measured on a precision source/measurement system. Au/AHO/TiN/SiO_2/Si MIM capacitors demonstrate capacitance density of 1.5 - 4.5 fF/μm^2 at 10 kHz, dielectric constant of 11.7 - 35.5 at 10 kHz, a loss tangent of 0.02 - 0.04 at 10 kHz, and leakage current density of 5.19×10^{-8} - 5.41×10^{-6} A/cm^2 at 1 MV/cm at room temperature.

Our results demonstrate sufficiently low leakage and high capacitance of compositional AHO thin film Capacitors and suggest the possible use of these MIM Capacitors in microelectronic applications which can be attributed to the following three factors. First, high temperature ALD growth of compositional AHO films results in the possibility of preferential (200)-oriented but multi-phase films without extra annealing process. However, single tetragonal phase with annealing process (up to 1700˚C) would be expected better electrical properties. Second, supplementation of Al_2O_3 into HfO_2 system showed better dielectric properties of films grown on TiN coated SiO_2/Si substrates, thereby achieving the formation of independent high-*k* thin film with semi metal electrode. Third, owing to smooth combination of materials mixture, I - V analysis indicated relatively low leakage current and low loss of composited dielectric layer comparable with laminated structured. However, complementary studies for the structure of TiN/AHO/TiN/SiO_2/Si with all-in-one thin film process without vacuum break are essential for an in-depth analysis of the correlation between electrical properties and smooth interfaces. Finally, this experimental approach to the different types of compositional thin films could be a challenging in the field of thin film dielectrics with ALD technique and could be served as a potential guideline to achieve high density capacitance and low leakage oxide layer in the future semiconductor processing.

Fund

This work was supported by the National Key R&D Program of China (Contract No. 2017YFA0305400), Natural Science the National Natural Science Foundation of China (Grant No. 61874073) and Ultimate High-*k* challenge project in Quantum Device Laboratory.

Conflicts of Interest

The authors declare no conflicts of interest regarding the publication of this paper.

References

[1] Wilk, G.D., Wallace, R.M. and Anthony, J. (2001) High-K Gate Dielectrics: Current Status and Materials Properties Considerations. *Journal of Applied Physics*, **89**, 5243-5275. https://doi.org/10.1063/1.1361065

[2] Schaller, R.R. (1997) Moore's Law: Past, Present and Future. *IEEE Spectrum*, **34**, 52-59. https://doi.org/10.1109/6.591665

[3] Robertson, J. and Wallace, R.M. (2015) High-K Materials and Metal Gates for CMOS Applications. *Material Science and Engineering R*: *Report*, **88**, 1-41. https://doi.org/10.1016/j.mser.2014.11.001

[4] Robertson, J. (2004) High Dielectric Constant Oxides. *European Physical Journal Applied Physics*, **28**, 265-291. https://doi.org/10.1051/epjap:2004206

[5] Gutowski, M., Jaffe, J.E., Liu, C.L., Stoker, M., Hegde, R.I., Rai, R.S. and Tobin, P.J. (2002) Thermodynamic Stability of High-K Dielectric Metal Oxides ZrO_2 and HfO_2 in Contact with Si and SiO_2. *Applied Physics Letter*, **80**, 1897-1899. https://doi.org/10.1063/1.1458692

[6] Tucker, J.R., Wang, C. and Carney, P.S. (1994) Silicon Field Effect Transistor Based on Quantum Tunneling. *Applied Physics Letter*, **65**, 618-620. https://doi.org/10.1063/1.112250

[7] Balog, M., Schieber, M., Michman, M. and Patai, S. (1977) Chemical Vapor Deposition and Characterization of HfO_2 Films from Organo-Hafnium Compounds. *Thin Solid Films*, **41**, 247-259. https://doi.org/10.1016/0040-6090(77)90312-1

[8] Kim, K.-M., Jang, J.S., Yoon, S.-G., Yun, J.-Y. and Chung, N.-K. (2020) Structural, Optical and Electrical Properties of HfO_2 Thin Films Deposited at Low-Temperature Using Plasma-Enhanced Atomic Layer Deposition. *Materials*, **13**, Article No. 2008. https://doi.org/10.3390/ma13092008

[9] Nishide, T., Honda, S., Matsuura, M. and Ide, M. (2000) Surface, Structural and Optical Properties of Sol-Gel Derived HfO_2 Films. *Thin Solid Films*, **371**, 61-65. https://doi.org/10.1016/S0040-6090(00)01010-5

[10] Heuer, A.H., Zahiri Azar, M., Guhl, H., Foulkes, M., Gleeson, B., Nakagawa, T., Ikuhara, Y. and Finnis, M.W. (2016) The Band Structure of Polycrystalline Al_2O_3 and Its Influence on Transport Phenomena. *Journal of the American Ceramic Society*, **99**, 733-747. https://doi.org/10.1111/jace.14149

[11] Afanas'ev, V.V., Houssa, M., Stesmans, A., Merckling, C., Schram, T. and Kittl, J.A. (2011) Influence of Al_2O_3 Crystallization on Band Offsets at Interfaces with Si and TiN_x. *Applied Physics Letter*, **99**, Article ID: 072103. https://doi.org/10.1063/1.3623439

[12] Tan, Y.N., Chim, W.K., Choi, W.K., Joo, M.S. and Cho, B.J. (2006) Hafnium Aluminum Oxide as Charge Storage and Blocking-Oxide Layers in SONOS-Type Nonvolatile Memory for High-Speed Operation. *IEEE Transactions on Electronic Device*, **53**, 654-662. https://doi.org/10.1109/TED.2006.870273

[13] Edlmayr, V., Moser, M., Walter, C. and Mitterer, C. (2009) Thermal Stability of Sputtered Al_2O_3 Coatings. *Surface and Coatings Technology*, **204**, 1576-1581. https://doi.org/10.1016/j.surfcoat.2009.10.002

[14] Birey, H. (1997) Thickness Dependence of the Dielectric Constant and Resistance of Al_2O_3 Films. *Journal of Applied Physics*, **48**, 5209-5212. https://doi.org/10.1063/1.323603

[15] Johnson, R.S., Hong, J.G., Hinkle, C. and Lucovsky, G. (2002) Electron Trapping in Noncrystalline Remote Plasma Deposited Hf-Aluminate Alloys for Gate Dielectric Applications. *Journal of Vacuum Science & Technology B*, **20**, 1126-1131.

https://doi.org/10.1116/1.1481872

[16] Kukli, K., Kemell, M., Castán, H., Dueñas, S., Seemen, H., Rähn, M., Link, J., Stern, R., Ritala, M. and Leskelä, M. (2018) Atomic Layer Deposition and Properties of HfO_2-Al_2O_3 Nanolaminates. *ECS Journal of Solid State Science and Technology*, **7**, 501-508. https://doi.org/10.1149/2.0261809jss

[17] Yu, H.Y., Li, M.F., Cho, B.J., Yeo, C.C., Joo, M.S. and Kwong, D.-L. (2002) Energy Gap and Band Alignment for $(HfO_2)_x(Al_2O_3)_{1-x}$ on (100)Si. *Applied Physics Letter*, **81**, 376-378. https://doi.org/10.1063/1.1492024

[18] Sen, B., Wong, H., Filip, V., Choi, H.Y., Sarkar, C.K., Chan, M., Kok, C.W. and Poon, M.C. (2006) Current Transport and High-Field Reliability of Aluminum/Hafnium Oxide/Silicon Structure. *Thin Solid Films*, **504**, 312-316. https://doi.org/10.1016/j.tsf.2005.09.052

[19] Buiu, O., Lu, Y., Hall, S., Mitrovic, I.Z., Potter, R.J. and Chalker, P.R. (2007) Investigation of Optical and Electronic Properties of Hafnium Aluminate Films Deposited by Metal-Organic Chemical Vapour Deposition. *Thin Solid Films*, **515**, 3772-3778. https://doi.org/10.1016/j.tsf.2006.09.035

[20] Wang, L.-G., Qian, X., Cao, Y.-Q., Cao, Z.-Y., Fang, G.-Y., Li, A.-D. and Wu, D. (2015) Excellent Resistive Switching Properties of Atomic Layer-Deposited Al_2O_3/HfO_2/Al_2O_3 Trilayer Structures for Non-Volatile Memory Applications. *Nanoscale Research Letters*, **10**, Article No. 135. https://doi.org/10.1186/s11671-015-0846-y

[21] Li, M., Jin, Z.-X., Zhang, W., Bai, Y.-H., Cao, Y.-Q., Li, W.-M., Wu, D. and Li, A.-D. (2019) Comparison of Chemical Stability and Corrosion Resistance of Group IV Metal Oxide Films Formed by Thermal and Plasma-Enhanced Atomic Layer Deposition. *Scientific Reports*, **9**, Article No. 10438. https://doi.org/10.1038/s41598-019-47049-z

[22] Molas, G., Bocquet, M., Buckley, J., Grampeix, H., Gely, M., Colonna, J.-P., Licitra, C., Rochat, N., Veyront, T., Garros, X., Martin, F., Brianceau, P., Vidal, V., Bongiorno, C., Salvo, B.D. and Deleonibus, S. (2007) Investigation of Hafnium-Aluminate Alloys in View of Integration as Interpoly Dielectrics of Future Flash Memories. *Solid State Electronics*, **51**, 1540-1546. https://doi.org/10.1016/j.sse.2007.09.020

[23] Cullity, B.D. and Stock, S.R. (2001) Elements of X-Ray Diffraction. 3rd Edition, Prentice-Hall, Upper Saddle River, 337-340.

[24] Meena, J.S., Chu, M.C., Kuo, S.W., Chang, F.C. and Ko, F.H. (2010) Improved Reliability from a Plasma-Assisted Metal-Insulator-Metal Capacitor Comprising a High-K HfO_2 Film on a Flexible Polyimide Substrate. *Physical Chemistry Chemical Physics*, **12**, 2582-2589. https://doi.org/10.1039/b917604g

[25] Sudo, Y., Hagiwara, M. and Fujihara, S. (2016) Grain Size Effect on Electrical Properties of Mn-Modified $0.67BiFeO_3$-$0.33BaTiO_3$ Lead-Free Piezoelectric Ceramics. *Ceramic International*, **42**, 8206-8211. https://doi.org/10.1016/j.ceramint.2016.02.030

[26] Wang, Y., Chen, Y., Zhang, Y., Zhu, Z., Wu, T., Kou, X., Ding, P., Corcolle, R. and Kim, J. (2021) Experimental Characterization of ALD Grown Al_2O_3 Film for Microelectronic Applications. *Advances in Materials Physics and Chemistry*, **11**, 7-19. https://doi.org/10.4236/ampc.2021.111002

[27] Gusev, E.P., Cartier, E., Buchanan, D.A., Gribelyuk, M., Copel, M., Okorn-Schmidt, H. and D'Emic, C. (2001) Ultrathin High-K Metal Oxides on Silicon: Processing, Characterization and Integration Issues. *Microelectronic Engineering*, **59**, 341-349. https://doi.org/10.1016/S0167-9317(01)00667-0

[28] Zhao, X. and Vanderbilt, D. (2002) First-Principles Study of Structural, Vibrational,

and Lattice Dielectric Properties of Hafnium Oxide. *Physics Review B*, **65**, Article ID: 075105. https://doi.org/10.1103/PhysRevB.65.075105

[29] Payne, A., Brewer, O., Leff, A., Strnad, N.A., Jones, J.L. and Hanrahan, B. (2020) Dielectric, Energy Storage, and Loss Study of Antiferroelectric-Like Al-Doped HfO_2 Thin Films. *Applied Physics Letter*, **117**, Article ID: 221104. https://doi.org/10.1063/5.0029706

[30] Lin, J., Masaaki, N., Tsukune, A. and Yamada, M. (1999) Ta_2O_5 Thin Films with Exceptionally High Dielectric Constant. *Applied Physics Letter*, **74**, 2370-2372. https://doi.org/10.1063/1.123854

[31] Desu, C.S., Joshi, P.C. and Desu, S.B. (2003) The Enhanced Dielectric and Insulating Properties of Al_2O_3 Modified Ta_2O_5 Thin Films. *Journal of Electroceramics*, **10**, 209-214. https://doi.org/10.1023/B:JECR.0000011219.91180.4c